Summary Report 2020
Phytoplankton and Zooplankton Monitoring at Sample Sites FSH-MG, PRI-UP, SPG, WEA, and WT-S

PREPARED FOR:

Three Rivers Park District
12615 Rockford Road
Plymouth, MN 55441
(763) 694-2061

PREPARED BY:

BSA Environmental Services, Inc.
23400 Mercantile Rd., Suite 8
Beachwood, OH 44122

POINT OF CONTACT:

John R. Beaver, Ph.D.
(216) 765-0582
j.beaver@bsaenv.com

2 MARCH 2021

Three Rivers Park District: Summary Report 2020 for Phytoplankton and Zooplankton Monitoring at FSH-MG, PRI-UP, SPG, WEA, and WT-S

1. Objective

In lake ecosystems phytoplankton form the base of aquatic food webs, while zooplankton function as key intermediaries of energy transfer between primary producers and fish. Both phytoplankton and zooplankton are highly sensitive to changes in water quality and can thus serve as indicators of overall ecological health in aquatic systems. Analyses of spatial distribution of specific taxa, as well as relative abundance and biomass, allow park district managers to assess the availability of important food web resources and to determine whether any water quality concerns need to be addressed.

The purpose of this report is to summarize phytoplankton and zooplankton seasonal dynamics from four sites (FSH-MG, PRI-UP, WEA, and WT-S) within the Three Rivers Park District (Minnesota, USA) during the spring, summer, and early fall of 2020. Results are compared across the four sites within the sampling period. An additional site (SPG) was sampled once for phytoplankton in order to determine the cause of water discoloration. The relative influence of important water quality variables (surface water temperature, total nitrogen and phosphorus concentrations, specific conductivity and water clarity) on phytoplankton and zooplankton community dynamics is assessed.

2. Methods

2.1 Field Methods

Five sites within the Three Rivers Park District (FSH-MG, PRI-UP, SPG, WEA, and WT-S) were sampled for this study. Four sites (FSH-MG, PRI-UP, WEA, and WT-S) were sampled approximately monthly for six months, beginning in April 2020 and ending in September 2020 (Table 1). Samples were collected from three sites (FSH-MG, WEA, and WT-S) on the same day for each sampling event, thus allowing direct comparison across sites. PRI-UP was sampled the day after the previous three sites. Site SPG was sampled only once on May 5, 2020 and only a phytoplankton sample was taken.

Phytoplankton samples were collected using a 2-meter composite tube at the surface. Two pulls were taken for each sampling event and homogenized in a large sample jug before pouring into 250 ml HDPE sample bottles. Samples were preserved immediately following collection using Lugol's iodine solution.

Zooplankton were collected using a Wisconsin-style mesh net with a diameter of 12.7 centimeters. Vertical tows for zooplankton samples were performed to a depth of 13 to 14 m at FSH-MG, 12 m at site WT-S, 15 to 16 m at site WEA, and 6 to 7 m at site WT-S. The samples were rinsed with lake water into the cod end of the net, which was then rinsed into 250 ml HDPE sample bottles. Zooplankton samples were preserved with Lugol's iodine solution, then capped and sealed to prepare for shipment.

Phytoplankton and zooplankton sample bottles were shipped to BSA Environmental Services, Inc. (Beachwood, OH, USA) for identification and enumeration. Water quality variables including temperature (°C), dissolved oxygen (% and mg L^{-1}), pH, specific

conductivity (µS cm^{-1}), total phosphorus (µg L^{-1}), soluble reactive phosphorus (µg L^{-1}), total nitrogen (mg L^{-1}), and chlorophyll-a (µg L^{-1}) were collected at the surface (0 m depth), as well as at each meter to the bottom of the sampling site. Secchi depth (m), a measure of water clarity, was recorded at each sampling event using a standard, black and white Secchi disk.

Table 1: 2020 Sampling dates for each site.

	FSH-MG	PRI-UP	SPG	WEA	WT_S
April	4/20/20	4/21/20		4/20/20	4/20/20
May	5/18/20	5/19/20	5/5/20*	5/18/20	5/18/20
June	6/15/20	6/2/20		6/15/20	6/15/20
		6/16/20			
July	7/13/20	7/14/20		7/13/20	7/13/20
August	8/10/20	8/11/20		8/10/20	8/10/20
September	9/8/20	9/9/20		9/8/20	9/8/20

*Only one phytoplankton sample from 5/5/20 was sent from sample site SPG for the 2020 season.

2.2 *Laboratory Methods*

2.2.1 Phytoplankton

Phytoplankton samples were processed using the membrane filtration technique (McNabb 1960). Sample bottles were gently homogenized and then various aliquots were concentrated onto a cellulose filter using vacuum filtration at low pressure. Filters were then soaked in immersion oil for transparency and adhered to glass slides for examination.

Phytoplankton were identified down to the lowest possible taxonomic level, usually species, using a Leica DMLB compound microscope. Organisms were counted in random fields up to a tally of 400 natural units (colonies, filaments and unicells) at 630X magnification, followed by an entire strip on the widest part of the filter to capture large and/or rare taxa that were not counted in the random fields.

Phytoplankton biovolume (µm^3 L^{-1}) was estimated on an individual cell basis using formulae for solid geometric shapes that most closely match the cell shape (Hillebrand et al., 1999). For the purposes of this report, nomenclature was updated to the most recent valid taxonomic classification scheme. Notably, all species identified under the genus *Anabaena* are referred to in this report as *Dolichospermum* (Wacklin et al. 2009). All species previously identified under *Cylindrospermopsis* are now classified as *Raphidiopsis* (Aguilera et al. 2018). Updates to divisions were also included in this year's report. The division Miozoa was previously reported as Pyrrophyta (Cavalier-Smith 1987). The divisions Ochrophyta and Haptophyta were both previously classified under Chrysophyta (Cavalier-Smith 1986, Cavalier-Smith & Chao, 1996). Charophyta was previously classified under Chlorophyta (Womersley 1984).

2.2.2 Zooplankton

Zooplankton samples were identified and enumerated using the Utermöhl sedimentation technique (Utermöhl 1958) and were examined at 100X magnification using a Leica DMi1 inverted microscope. For each sample, zooplankton were quantified and identified to the lowest practical taxon, usually species, with a minimum count of 200 organisms. The lengths of all observed taxa were measured using class-specific guidelines (Dumont et al. 1975, McCauley 1984, Lawrence et al. 1987). Up to ten individuals of each identified species were measured. Density was estimated as organisms L^{-1} based on the volume of water sampled for each vertical tow. Biomass was estimated as micrograms of dry weight per liter (μg d.w. L^{-1}) for specific genera and species using established length-mass relationships (Dumont et al. 1975, McCauley 1984, Lawrence et al. 1987).

2.3 *Multivariate Analyses*

Canonical correlation analyses (CCAs) were performed using the Canonical Analysis of Principal Coordinates (CAP) function of the PERMANOVA+ add-on in PRIMER v.7 software (Clarke & Gorley 2006). Samples from 2018 through 2020 were included in the CCA, and all matrices contained a total of n=64 samples. The phytoplankton sample from SPG collected in May 2020 was excluded from CCA due to missing environmental data. Three data matrices were prepared for these analyses.

- First matrix: consisted of water quality variables for each sample collected: water temperature (°C), specific conductivity (μS cm^{-1}), Secchi depth (m), total phosphorus (TP, μg L^{-1}), total nitrogen (TN, mg L^{-1}) and chlorophyll-a (μg L^{-1}). Only surface values (0 m depth) were included in this analysis.

- Second data matrix: comprised of total biovolume values (μm^3 L^{-1}) for each phytoplankton genus (94 genera) for each sample collected.

- Third data matrix: comprised of the zooplankton biomass (μg d.w. L^{-1}) value for all identified adult cladoceran and copepod species for each sample collected (excluding ostracods, rotifers, nauplii and juvenile taxa).

Prior to the analysis, the biological matrices (phytoplankton biovolume, zooplankton biomass) were standardized and a Bray-Curtis resemblance matrix was computed. The environmental matrix (water quality variables) was normalized in order to get all variables on a common scale. For CAP analysis, both the phytoplankton biovolume matrix and the zooplankton biomass matrix were individually analyzed against the sample-matched water quality matrix. Chlorophyll-a was removed from the set of water quality variables in the phytoplankton analysis, in order to prevent autocorrelation. Subsequent to the analysis, the biovolume/biomass of individual phytoplankton (*Aphanizomenon* spp. and *Dolichospermum* spp.) and zooplankton (*Daphnia galeata*, *D. pulex* and *D. retrocurva*) taxa were superimposed onto the respective CCA ordination plots.

3. Results

3.1 Phytoplankton seasonal dynamics

Of the five sites included in this study, FSH-MG showed the lowest phytoplankton biovolume and WT-S showed the highest biovolume throughout the sampling period compared to the other sites (Figure 1). Phytoplankton biovolume was lowest at FSH-MG (1.65×10^6 µm^3 L^{-1}) during the July 13, 2020 sampling event. The highest recorded biovolume (8.71×10^7 µm^3 L^{-1}) was recorded on the same sampling date on July 13, 2020 at WT-S. None of the three sites showed distinct increasing or decreasing trends in phytoplankton biomass over the course of the season.

Common cyanobacterial species observed from this study included the diazotrophic (nitrogen-fixing) species *Dolichospermum* spp., *Aphanizomenon* spp. and *Raphidiopsis* spp. (Figure 2), which are also capable of producing hepatotoxins (microcystins). *Planktothrix* spp. is a non-diazotrophic genus but also produces microcystins.

Common diatom (Bacillariophyta) species making large contributions to biovolume included *Asterionella formosa, Fragilaria* spp. and *Aulacoseira* spp. Common cryptophytes (Cryptophyta) included *Plagioselmis nannoplanctica* and *Cryptomonas* spp. Taxa in Chlorophyta (green algae), Charophyta, Chrysophyta and Ochrophyta did not make significant biovolume contributions to the phytoplankton community at any of the five sites.

3.1.1 FSH-MG

At sites FSH-MG, the majority of phytoplankton biovolume came from cyanobacteria later in the season (August/September), while earlier in the season the phytoplankton community was dominated by Bacillariophyta (April/May) and Ochrophyta (June). The cyanobacteria community at FSH-MG consisted mostly of *Aphanizomenon* spp. throughout the season, however *Raphidiopsis* spp. was dominant at that site during the September 8 sampling event (Table 2). Relative contribution of cyanobacteria was highest at FSH-MG during August and September of 2020, which is slightly later in the season compared to 2018 and 2019 (Figure 3).

3.1.2 PRI-UP

Similar to FSH-MG, phytoplankton counts at PRI-UP showed that the majority of phytoplankton biovolume earlier in the season came from Bacillariophyta (April/May) and Ochrophyta (June), while cyanobacteria was dominant later in the season (August/September). Overall, PRI-UP showed higher biovolume than FSH-MG throughout the sampling season, despite similar seasonal community succession patterns. At PRI-UP *Aphanizomenon* spp. was the dominant cyanobacterial taxon in spring and early-mid summer, but in August and early September high biovolumes of both *Raphidiopsis* spp. and *Planktothrix* spp. were observed. Highest biovolumes of diatoms (Bacillariophyta) were observed at PRI-UP.

3.1.3 WEA

At sites WEA, the majority of phytoplankton biovolume came from cyanobacteria throughout the season. *Aphanizomenon* spp. was the dominant cyanobacterial taxon

throughout the 2020 sampling season. While in previous years, spring sampling events (May/June) were dominated by Cryptophyta, cyanobacteria were dominant as early as April in 2020 and remained high throughout the remainder of the summer.

3.1.4 WT-S

At WT-S, the majority of phytoplankton biovolume came from cyanobacteria throughout the season, although large contributions to biovolume by Cryptophyta were observed both in the spring (April) and late summer (September). High biovolume of Miozoa (dinoflagellates) was also observed at WT-S in mid-July, which came primarily from the species *Ceratium hirundinella.* Similarly to site PRI-UP, *Aphanizomenon* spp. was the dominant cyanobacterial taxon in spring and early-mid summer, but in August and early September high biovolumes of both *Raphidiopsis* spp. and *Planktothrix* spp. were observed. Like in previous years (2018 and 2019), relative cyanobacteria biovolume at WT-S was highest during July and August and then waned later by September.

3.1.5 SPG

The single sampling event at site SPG showed a mix of diatoms, cryptophyte and cyanobacteria, with minor contributions from other divisions. Both *Aphanizomenon* spp. and *Raphidiopsis* spp. were observed during the single sampling event at SPG.
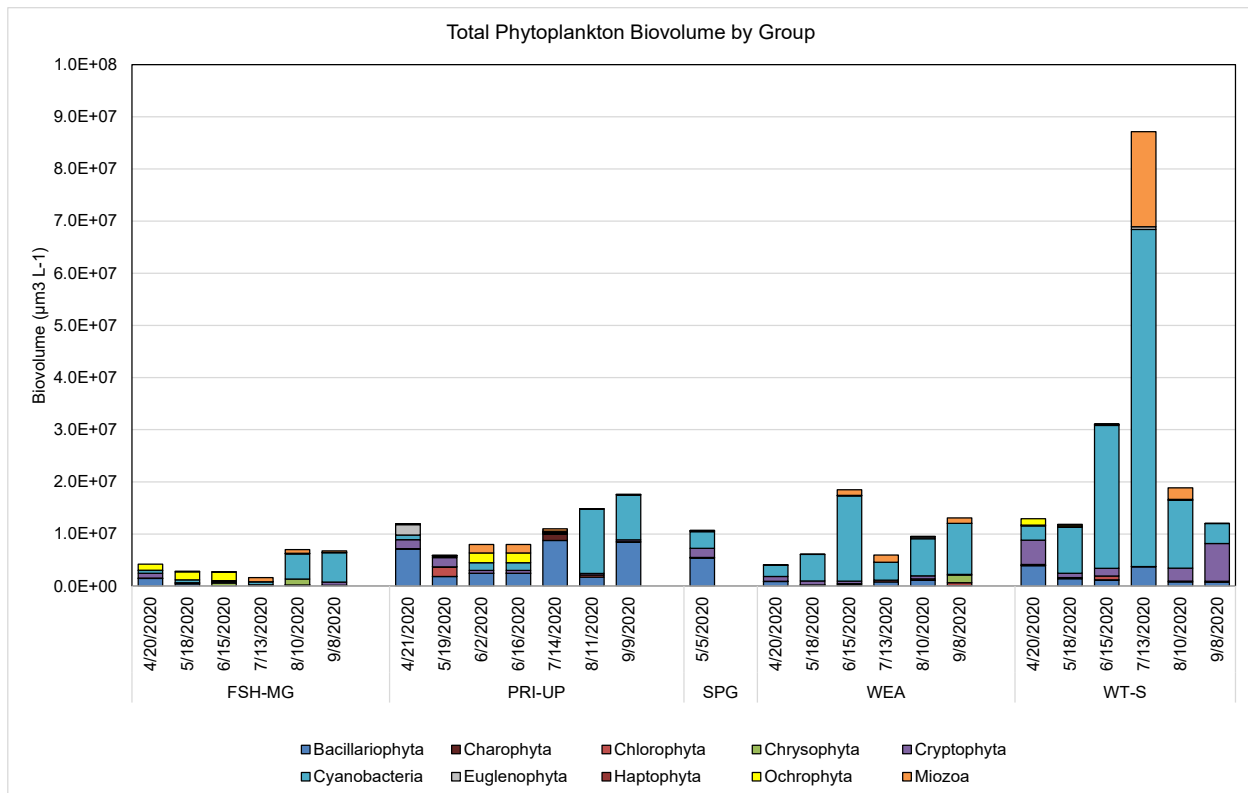

Figure 1: Total phytoplankton biovolume (μm^3 L^{-1}) by group at each sampling event for each of the five study sites in 2020. The division Miozoa was previously reported as Phyrrophyta. The divisions Ochrophyta and Haptophyta were both previously classified under Chrysophyta. Charophyta was previously classified under Chlorophyta.

Table 2: Percentage contribution of dominant potentially-toxigenic (microcystin-producing) cyanobacteria: *Dolichospermum sp.*, *Aphanizomenon sp.,* and Raphidiopsis spp. (previously classified as *Cylindrospermopsis spp.*) to total cyanobacteria biovolume at each sampling event for each of the five study sites.

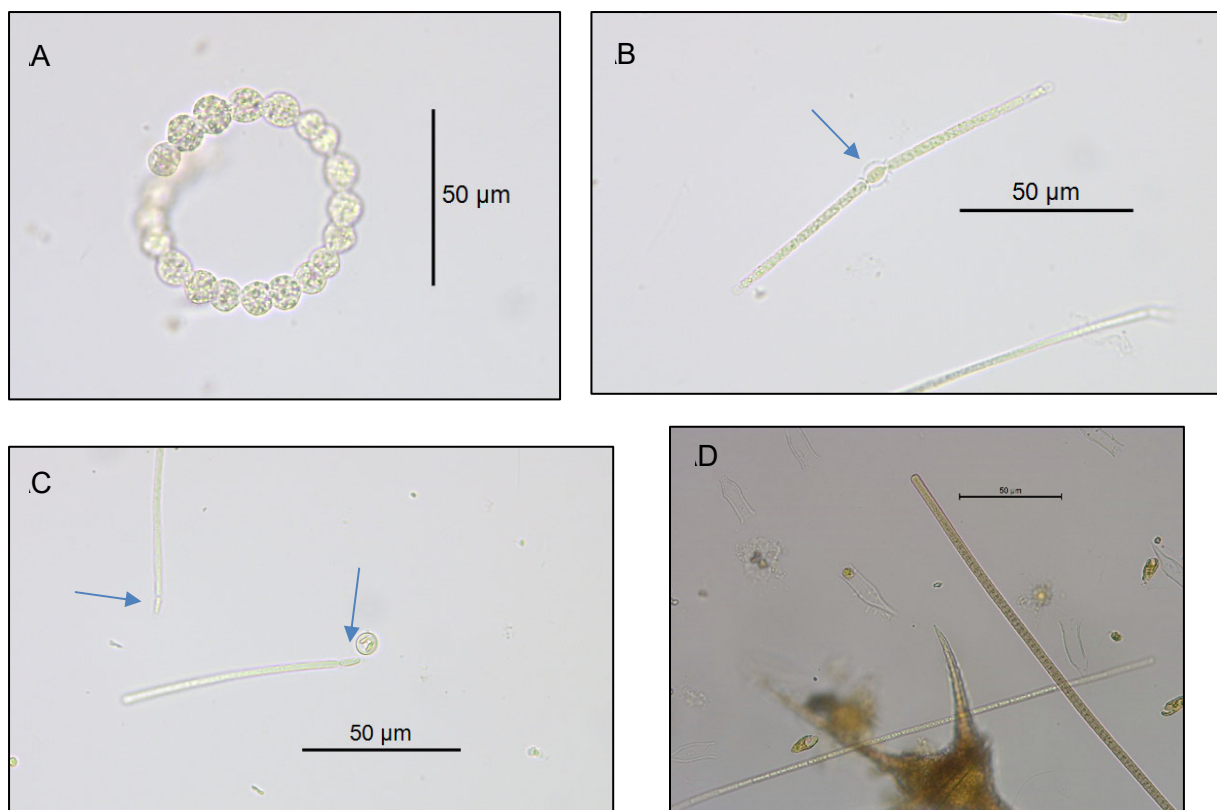|		*Dolichospermum* spp.	*Aphanizomenon* spp.	*Raphidiopsis* spp.	*Planktothrix* spp.
FSH-MG	4/20/2020			99.0%	
	5/18/2020		16.1%	83.1%	
	6/15/2020	2.3%	92.7%		
	7/13/2020	1.4%	59.9%		21.8%
	8/10/2020	9.7%	88.5%		
	9/8/2020		14.2%	77.7%	
PRI-UP	4/21/2020	0.3%	69.9%	28.7%	
	5/19/2020		95.8%	4.2%	
	6/2/2020	0.2%	26.1%	73.5%	
	6/16/2020	4.8%	24.4%		65.8%
	7/14/2020	6.0%	27.2%	14.7%	27.7%
	8/11/2020	0.2%	0.9%	63.3%	26.0%
	9/9/2020	0.2%		53.1%	43.7%
SPG	5/5/2020		35.4%	63.7%	
WEA	4/20/2020		83.4%	16.6%	
	5/18/2020	0.7%	88.1%		11.0%
	6/15/2020	1.9%	92.8%		
	7/13/2020	20.6%	74.5%		
	8/10/2020	10.7%	35.9%	0.8%	49.5%
	9/8/2020	47.4%	5.3%		
WT-S	4/20/2020		66.7%	32.0%	
	5/18/2020	8.1%	91.6%		
	6/15/2020	14.6%	76.8%		
	7/13/2020	5.6%	39.9%		25.7%
	8/10/2020	6.1%		92.5%	
	9/8/2020	4.3%		86.4%	

Figure 2: Microphotographs of dominant potentially toxigenic cyanobacteria. **A)** *Dolichospermum* sp. **B)** *Aphanizomenon* sp. **C)** *Raphidiopsis* sp. **D)** *Planktothrix* sp. Arrows indicate heterocytes (specialized nitrogen-fixing cells) on *Aphanizomenon* sp. and *Raphidiopsis* sp. *Photo Credits*: (A-C): C. Tausz, BSA Environmental Services, Inc. D: B. Bolam, BSA Environmental Services, Inc.
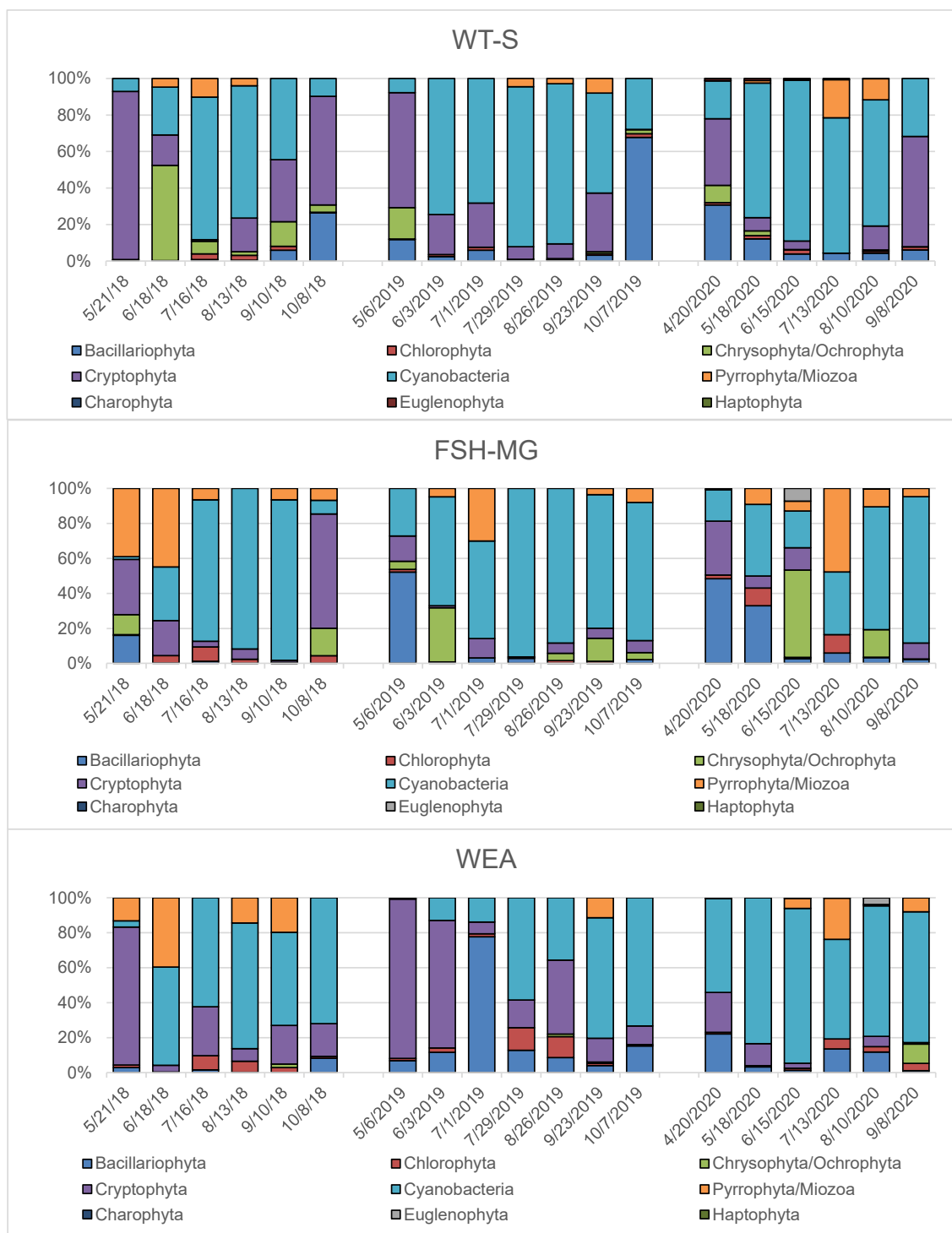
Figure 3: Relative phytoplankton biovolume by group at each sampling event for each of the three study sites sampled in 2018, 2019 and 2020. The divisions Chrysophyta and Ochrophyta, as well as Pyrrophyta and Miozoa were combined to reflect taxonomic synonyms.

3.2 Zooplankton seasonal dynamics

As with phytoplankton, the zooplankton community varied between the four sites and over the collection season (Figure 4). The highest cumulative zooplankton biomass over the course of the sampling season was observed at PRI-UP at 1908.41 µg d.w. L^{-1}. However, PRI-UP had an additional sampling event on June 2, 2020 following the addition of alum to the lake on May 26th-28th. Thus, this site had a total of seven sampling events for the season, more than any other site. The second highest cumulative zooplankton biomass over the course of six sampling events for the season was observed at FSH-MG at 1504.59 µg d.w. L^{-1}. WT-S showed the lowest cumulative zooplankton biomass in this study at 851.67 µg d.w. L^{-1}. All four sample sites, FSH-MG, PRI-UP, WEA, and WT-S, experienced relatively low total zooplankton biomass in July and August. Neither calanoid copepods nor nauplii (larval copepods) made significant contributions to biomass in any of the samples.

3.2.1 FSH-MG

At FSH-MG, high zooplankton biomass was observed earlier in the season from the April and May sampling events due to high densities of cyclopoida copepods (*Diacyclops thomasi and Mesocyclops edax*). However, in June high densities of the large cladoceran species *Daphnia galeata* and *Daphnia pulex* make up 78% of the zooplankton biomass (Table 3). In July, August, and September biomass densities were more evenly distributed between *Daphnia* spp. and cyclopoida copepod species (*Acanthocyclops robustus, Mesocyclops edax, Orthocyclops modestus,* and *Tropocyclops prasinus*). An increase in calanoid copepods was observed in September. Relative zooplankton biovolume patterns were similar in 2020 compared to previous years, however, notably, no *Daphnia* species were observed during April (not sampled in previous years) and August (Figure 5).

3.2.2 PRI-UP

At PRI-UP, WEA, and WT-S, relatively high zooplankton biomass was observed during the first half of the season primarily due to high densities of the large cladoceran species *Daphnia galeata, Daphnia pulex*, and *Daphnia retrocurva*. PRI-UP experienced particularly high *Daphnia* spp. biomass (999 µg d.w. L^{-1}) during the May 19, 2020 sampling event. PRI-UP also showed 49.8 µg d.w. L^{-1} of Rotifera, the highest relative Rotifera biomass (~42% of the total biomass) for the August 11, 2020 sample event. The only sample that recorded a higher total Rotifera biomass was FSH-MG (55.5 µg d.w. L^{-1}) on May 18, 2020.

3.3.3 WEA

Like PRI-UP, WEA saw relatively high zooplankton biomass during the first half of the season primarily due to high densities of large *Daphnia* spp. Interestingly however, *Daphnia* biomass was very low during the May 18. 2020 sampling event, while sampling events both a month prior (April 20, 2020) and a month afterwards (June 15, 2020) showed relatively high *Daphnia* biomass. This observation likely reflects the fast growth response that these organisms can show in response to both phytoplankton biomass and predation pressure. 2020 seasonal patterns in relative zooplankton biomass at WEA were similar to 2018 and 2019.

3.3.4 WT-S

WT-S saw the lowest total zooplankton biomass overall during the July 13, 2020 sampling event (0.2 µg d.w. L^{-1}), with the calanoid copepod *Skistodiaptomus oregonensis*

accounting for approximately half of the total observed biomass for that sample (0.12 µg d.w. L^{-1}). Additionally, WT-S recorded no *Daphnia* spp. in July, August, or September and no other cladocerans in August or September. The cyclopoid copepods *Mesocyclops edax* and *Tropocyclops prasinus* made up much of the total observed biomass at site WT-S in August (42.8 µg d.w. L^{-1}) and September (52.9 µg d.w. L^{-1}). As in 2019, WT-S saw high contributions to relative biomass by Cyclopoida throughout much of the sampling season.

3.3.5 Relationship to phytoplankton biovolume

At FSH-MG, PRI-UP, and WT-S, when zooplankton biomass was highest, phytoplankton biovolume was lowest in 2020 (Figure 6). In general, at those three sites, zooplankton biomass and phytoplankton biovolume showed opposite trends – where zooplankton biomass increased, phytoplankton biovolume decreased, and vice-versa. However, this trend did not hold true for WEA in 2020. While zooplankton biomass was highest and phytoplankton biovolume was lowest in April, both followed similar trends for the remainder of the sampling season.
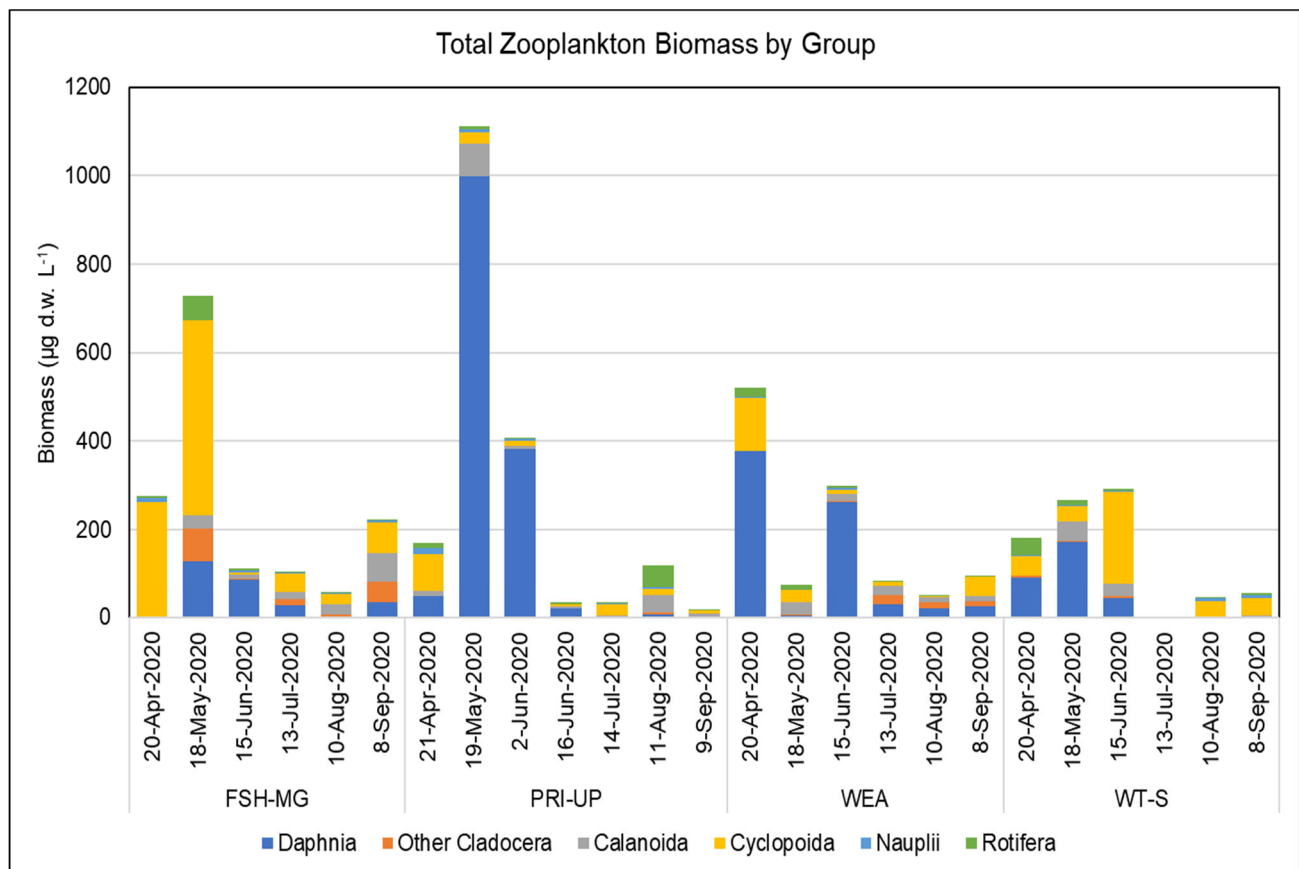

Figure 4: Total zooplankton biomass (µg d.w. L^{-1}) by group at each sampling event for each of the four study sites during the 2020 sampling season.

Table 3: Percentage contribution of total zooplankton biomass by (µg d.w. L^{-1}) group at each sampling event for each of the four study sites. Values greater than 50% are highlighted.

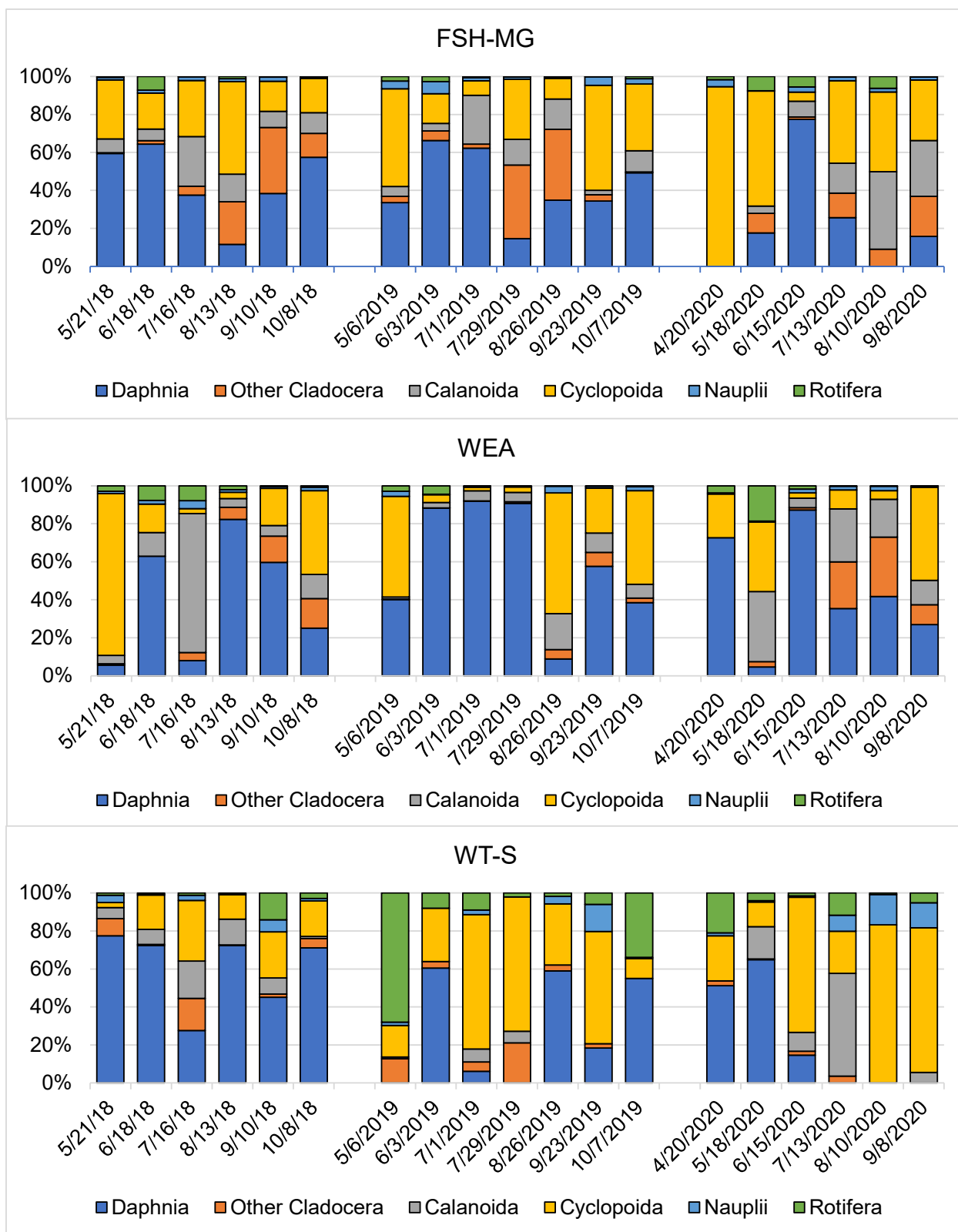|		*Daphnia*	Other Cladocera	Calanoida	Cyclopoida	Nauplii	Rotifera
FSH-MG	20-Apr-2020				94.5%	3.7%	1.8%
	18-May-2020	17.6%	10.2%	3.9%	60.5%	0.1%	7.6%
	15-Jun-2020	77.5%	1.1%	8.3%	4.9%	2.8%	5.5%
	13-Jul-2020	25.3%	12.8%	15.4%	42.8%	2.1%	0.2%
	10-Aug-2020	0.0%	9.1%	40.8%	41.9%	2.0%	6.2%
	8-Sep-2020	15.8%	21.1%	29.4%	31.8%	1.7%	0.3%
PRI-UP	21-Apr-2020	25.8%	0.0%	6.6%	47.6%	7.4%	5.7%
	19-May-2020	89.9%	0.0%	6.6%	2.3%	0.5%	0.6%
	2-Jun-2020	93.8%	0.0%	1.8%	3.0%	0.7%	0.7%
	16-Jun-2020	58.1%	0.0%	13.1%	17.0%	1.0%	10.0%
	14-Jul-2020	0.0%	2.7%	9.2%	59.5%	10.7%	2.6%
	11-Aug-2020	5.9%	2.4%	34.1%	10.6%	5.1%	41.9%
	9-Sep-2020	2.4%	3.0%	54.2%	30.8%	9.0%	0.6%
WEA	20-Apr-2020	72.6%	0.0%	0.0%	23.1%	0.6%	3.8%
	18-May-2020	4.7%	2.7%	37.0%	36.5%	0.5%	18.7%
	15-Jun-2020	87.3%	1.2%	5.0%	2.8%	2.1%	1.7%
	13-Jul-2020	35.4%	24.5%	27.9%	10.0%	1.9%	0.3%
	10-Aug-2020	41.7%	31.3%	19.9%	4.5%	2.3%	0.3%
	8-Sep-2020	26.6%	10.4%	12.6%	48.6%	0.6%	0.2%
WT-S	20-Apr-2020	51.2%	2.5%	0.0%	23.8%	1.5%	21.0%
	18-May-2020	63.4%	0.3%	16.7%	12.6%	0.7%	4.0%
	15-Jun-2020	14.3%	2.0%	9.7%	69.4%	0.7%	1.5%
	13-Jul-2020	0.0%	3.6%	54.3%	22.1%	8.4%	11.8%
	10-Aug-2020	0.0%	0.0%	0.0%	83.2%	16.0%	0.8%
	8-Sep-2020	0.0%	0.0%	5.5%	76.2%	13.2%	5.2%

Figure 5: Relative zooplankton biomass by group at each sampling event for each of the three study sites sampled during 2018, 2019 and 2020
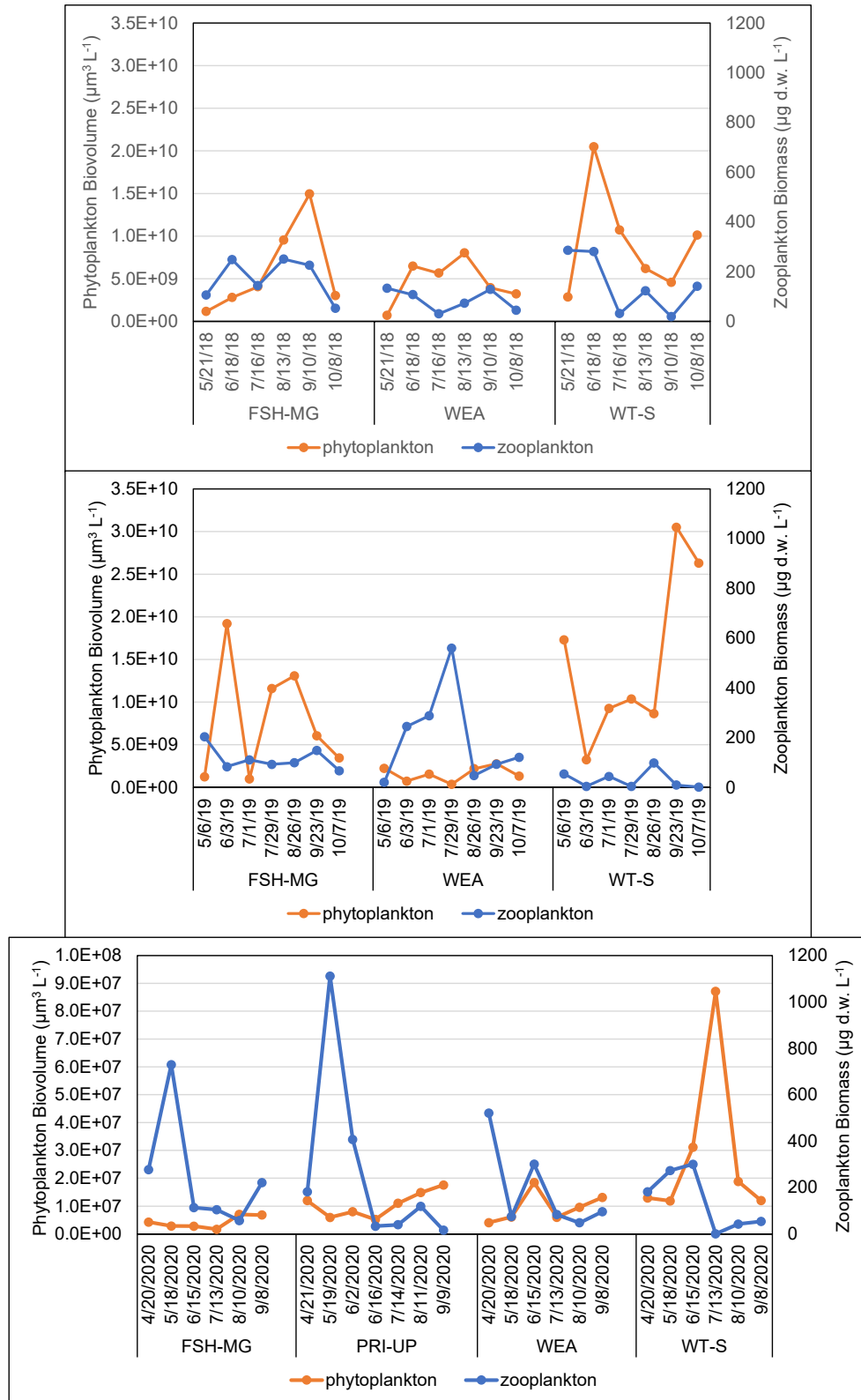
13

Figure 6: Total zooplankton biomass (µg d.w. L^{-1}) and total phytoplankton biovolume (µm^3 L^{-1}) at each sampling event for all study sites in 2018, 2019 and 2020. Note: scale difference for 2020 phytoplankton.

14

3.3 Environmental variables influencing phytoplankton and zooplankton communities

Multivariate statistical techniques such as CCA (Canonical Correlation Analysis) are analytical methods that delineate relationships between community structure and multiple environmental variables. CCA forms linear combinations of environmental variables that best explain the maximally separated patterns of inter-taxon density or biomass distribution (terBraak and Verdonschot 1995). The products of the CCA are canonical variables, which are multivariate linear functions of the original environmental and biological variables (Anderson and Willis 2003).

- Each sample used in the analysis is represented on the ordination by a single point that is given a score derived from the sample's correlation with the sources of variation. The analysis produces statistically independent canonical axes, called CAP axes, that represent the scoring system (coordinate system) based on environmental variables and the varying degrees of correlation with biovolume or biomass.

- Bubbles on the ordination diagrams the density or biomass for each sample, and the bubble position indicates the taxa preference in relation to the environmental variables. The relative placement of the bubbles on the ordination reflects similarities between density or biomass compositions.

- Lines (vectors) from the center of the ordination represent environmental variables with the line direction indicating a change in the environmental variable across the ordination, and the length of the line indicates the strength of the relationship.

For the phytoplankton biovolume CCA, the first two CAP axes explained 59 percent and 46 percent of variability in the data, respectively. The strongest environmental vectors were specific conductivity (ranging from 238 to 535 μS cm^{-1}) , water temperature (range of 7 to 28 $^\circ$C) and Secchi depth (range of 0.7 to 6.6 m), whereas both total nitrogen (range of 0.6 to 2.1 mg L^{-1}) and total phosphorus (range of 9.3 to 55.1 μg L^{-1}) had weak correlations to both axes. Specific conductivity showed a strong negative correlation to the CAP2 axis (-0.922). Water temperature showed a moderate negative correlation to the CAP1 axis (-0.572) and a moderate positive correlation to the CAP2 axis (0.324). Secchi depth was strongly positively correlated with the CAP1 axis (0.739), indicating an inverse relationship between water temperature and water clarity.

Superimposition of biovolume values for *Aphanizomenon* spp. and *Dolichospermum* spp. revealed different associations between the two taxa and concurrent water quality parameters, as well as differences in site locations (Figure 7). Highest biovolumes for *Aphanizomenon* spp. were observed on the negative side of the CAP2 axis, in association with high conductivity, cooler water temperatures and lower nutrients. Although *Aphanizomenon* spp. was present in sites WEA, FSH-MG and WT-S, biovolumes were highest in FSH-MG. In contrast, highest biovolumes for *Dolichospermum* spp. were observed on the positive side of CAP2, suggesting an association with warmer water temperatures and lower conductivity. Higher biovolumes of *Dolichospemum* spp. were observed in WEA and WT-S, while low biovolumes were observed in FSH-MG. This suggests that *Aphanizomenon* spp. is able to outcompete *Dolichospermum* spp. in FSH-MG. *Raphidiopsis* spp. was observed in both FSH-MG and WT-S, but not in WEA. Highest

biovolumes for *Raphidiopsis* spp. were associated with warmer temperatures, higher conductivity and decreased water clarity.

For the zooplankton biomass CCA, the first two CAP axes explained 58 percent and 47 percent of variability in the data, respectively. These values represent an improvement in the relationship between zooplankton biomass and water quality compared to the previous year (53 and 21 percent, respectively, in 2019). As with phytoplankton, the strongest vectors for the zooplankton biomass CCA were specific conductivity, water temperature and Secchi depth. Additionally, chlorophyll-a (representative of total phytoplankton biomass) also exhibited a strong relationship with zooplankton biomass. Both total nitrogen and total phosphorus were weakly correlated with zooplankton biomass. Specific conductivity, water temperature and Secchi depth all showed negative correlations to the CAP1 axis (-0.549, -0.559 and -0.312 respectively). Water temperature also showed a positive correlation to the CAP1 axis (0.699). Chlorophyll-a showed moderate positive correlations to both the CAP1 and the CAP2 axis (0.491 and 0.460 respectively).

Superimposition of biomass values onto the ordination diagram revealed differing preferences for water quality conditions between three species of *Daphnia*, a keystone herbivore in lake ecosystems (Figure 8). *Daphnia galeata* showed highest biomass values on the negative side of both CAP1 and CAP2, in association with high conductivity, increased water clarity and low chlorophyll-a. *Daphnia pulex* also showed high biomass values on the negative sides of CAP1 and CAP2. *Daphnia galeata* was observed with substantial biomass at all four study sites, while *Daphnia pulex* was observed at highest biomass in WEA and PRI-UP, with little to no biomass observed in FSH-MG and WT-S. *Daphnia retrocurva* was observed at all sites (although lowest biomass was observed at PRI-UP), without clear associations with water quality variables.
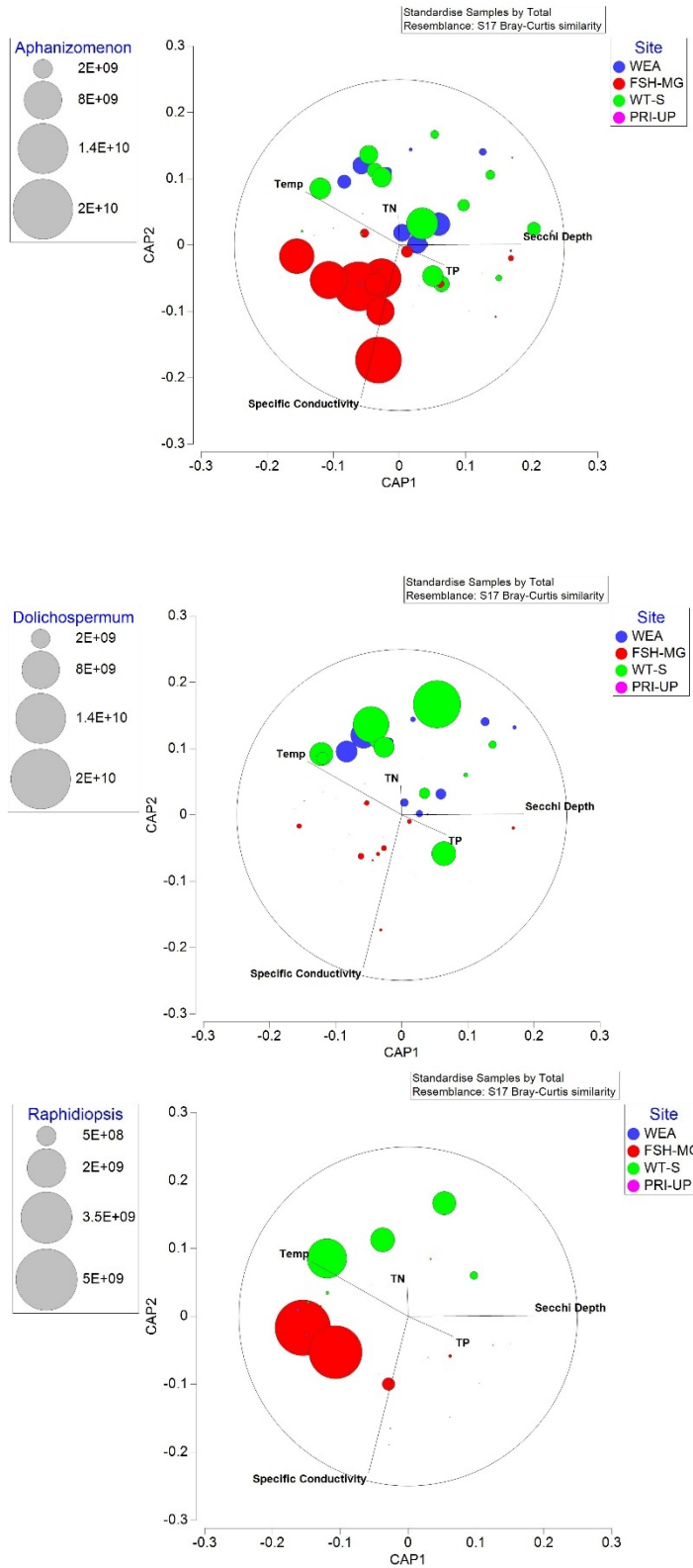
Figure 7: CCA ordination diagrams showing biovolume (µm^3 L^{-1}) values for *Aphanizomenon* spp. (top), *Dolichospermum* spp. (middle) and *Raphidiopsis* spp. (bottom). Each bubble represents a single sample and bubble size represents the magnitude of biovolume within that sample. Bubble color represents site location.
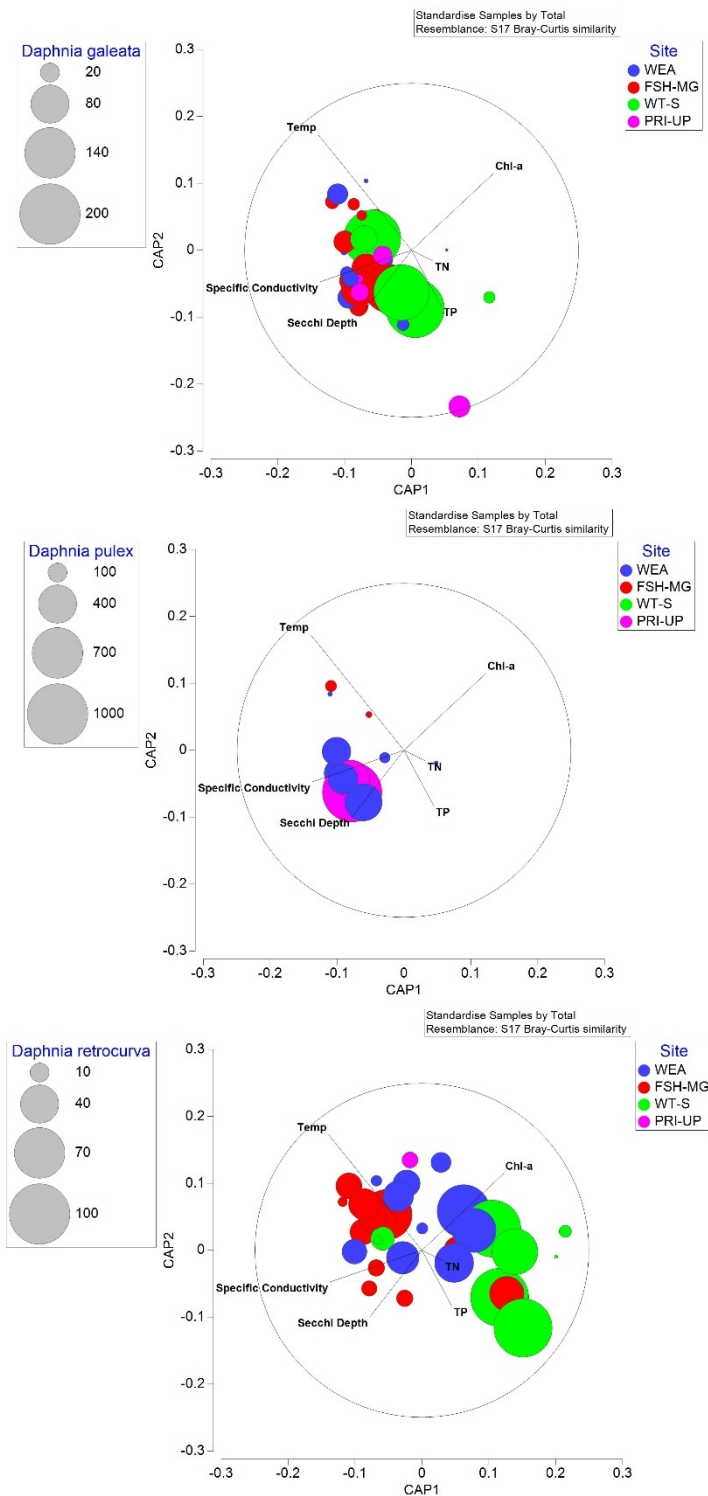
17

Figure 8: CCA ordination diagrams showing biomass (µg d.w. L^{-1}) values for *Daphnia galeata* (top), *Daphnia pulex* (middle) and *Daphnia retrocurva* (bottom). Each bubble represents a single sample and bubble size represents the magnitude of biovolume within that sample. Bubble color represents site location.

18

4. Discussion

All four sites that were sampled throughout the season within the Three Rivers Parks District saw dominance of cyanobacteria species within the phytoplankton community during the summer and early fall of 2020. Higher phytoplankton diversity – as observed at FSH-MG and PRI-UP in the spring and early summer – is indicative of better ecosystem health, as cyanobacteria are generally considered lower quality food sources for grazing zooplankton due to their relatively low lipid content.

Many species of cyanobacteria are also able to produce toxins as secondary metabolites, which can negatively impact lake ecosystems at higher trophic levels and cause adverse effects on human health and recreation. High growth rates and high biomass are often positively correlated with the degree of toxin production. All four of the major cyanobacterial taxa – *Aphanizomenon*, *Dolichospermum, Raphidiopsis* and *Planktothrix* – are potential toxin producers. Three of these taxa (*Aphanizomenon*, *Dolichospermum* and *Raphidiopsis*) are also diazotrophic and produce specialized nitrogen-fixing cells (heterocytes). The fact that the major cyanobacterial taxa are diazotrophic indicates that nitrogen is the limiting nutrient for non-diazotrophic phytoplankton in these systems, while phosphorus is the limiting nutrient for species with nitrogen-fixing capabilities. Diazotrophic taxa are typically able to outcompete other phytoplankton species when nitrogen is scarce, provided there is a sufficient amount of phosphorus available for growth.

Despite the known relationship between nutrients and phytoplankton growth (and potential toxin production), CCA amongst phytoplankton taxa showed that nutrient concentrations were not strongly correlated to phytoplankton community composition. Instead, environmental variables such as water temperature, conductivity and water clarity showed stronger relationships with cyanobacterial dominance. This result suggests that dominant cyanobacterial taxa were able to take advantage of warm and clear conditions (typical of a stratified lake during the summer months in a temperate climate) to outcompete other phytoplankton taxa, whose biovolume may have been diminished as a result of early season zooplankton grazing.

At all four sites sampled for zooplankton, biomass was highest in spring (April) and early summer (May and June), then declined throughout the later summer. High zooplankton biomass was generally associated with low phytoplankton biovolume. Inverse trends between total zooplankton biomass and total phytoplankton biovolume indicate that grazing efficiency of *Daphnia* and other large zooplankton was high enough to effectively crop phytoplankton standing stock. Less palatable, faster-growing cyanobacteria species were likely able to take advantage of mid-summer conditions after zooplankton had grazed the majority of slower-growing, more nutritionally-dense phytoplankton species, when total zooplankton biomass was declining.

Given that high biovolumes of potentially toxigenic cyanobacteria have been observed over the course of three summers, it is suggested that testing for toxins (microcystins) might be of value to managers, particularly in areas of the lakes that are frequented for recreational activities (swimming, boating, fishing, etc.). Not all strains of potentially toxigenic taxa will produce toxins, however toxic and non-toxic strains of the same species are usually morphologically identical and further testing (beyond species-identification) is needed to determine toxicity in real time. This may be accomplished via PCR testing for the presence of microcystin-producing genes.

Although nutrient concentrations (total nitrogen and total phosphorus) were weakly correlated with phytoplankton community composition, a focus on reducing nutrient inputs into these lakes would likely have the most impact on disrupting growth of potentially toxigenic species. Temperate lakes naturally warm and stratify during summer months, creating favorable conditions for cyanobacterial growth. Management of cyanobacterial blooms may be complicated on a grand scale, and strategies may need to be tailored to specific locations. *Aphanizomenon* and *Dolichospermum* show dominance in separate sites and time periods within these lake ecosystems (see Figure 7), suggesting that changing environmental conditions (both seasonally and interannually) could result in varied growth responses between these two taxa. Additionally, the non-diazotrophic genus *Planktothrix* is typically more tolerant of reduced light availability (de Araujo Torres et al. 2015) and may have a different response to nutrient reductions than nitrogen-fixing taxa.

Comparisons of observations at all four lakes indicate that *Daphnia* species and other large zooplankton may exert top-down control on phytoplankton communities and may influence the timing of cyanobacterial blooms. Although moderate correlations to measured environmental variables were observed for the zooplankton community, other factors (such as top-down control via fish predation) likely play a role in controlling zooplankton populations. *Daphnia* specifically tend to be the preferred prey-item of planktivorous fish (Hall et al. 1976). Controlling fish populations in these lakes, particularly in spring and early summer, may contribute to higher *Daphnia* biomass and consequently a reduction of phytoplankton biovolume throughout the season. As plankton community dynamics can vary quite a bit from year to year, continued monitoring of these sites for phytoplankton, zooplankton and environmental quality variables is recommended.

5. References

Aguilera, A., E. Berrendero Gómez, J. Kastovsky, R. O. Echenique & G. L. Salerno, 2018. The polyphasic analysis of two native *Raphidiopsis* isolates supports the unification of *Raphidiopsis* and *Cylindrospermopsis* (Nostocales, Cyanobacteria). Phycologia 57: 130–146.

Anderson, M. J. & T. J. Willis, 2003. Canonical analysis of principal coordinates: a useful method of constrained ordination for ecology. Ecology 84: 511–525.

Cavalier-Smith, T. 1986. The kingdom Chromista: origin and systematics. Progress in Phycological Research 4, 309–347.

Cavalier-Smith, T. 1987. The origin of eukaryote and archaebacterial cells. Annals of the New York Academy of Sciences 503: 17–54.

Cavalier-Smith, T., & Chao, E. E. 1996. 18S rRNA sequence of Heterosigma carterae (Raphidophyceae), and the phylogeny of heterokont algae (Ochrophyta). Phycologia 35: 500–510.

Clarke, K. R. & R. N. Gorley. 2006. PRIMER v6: User Manual/Tutorial. PRIMER-E, Plymouth.

de Araujo Torres, C., M. Lürling & M. M. Marinho, 2016. Assessment of the effects of light availability on growth and competition between strains of *Planktothrix agardhii* and *Microcystis aeruginosa*. Microbial Ecology 71: 802–813.

Dumont, H. J., I. Van De Velde & S. Dumont, 1975. The dry weight estimate of biomass in a selection of Cladocera, Copepoda and Rotifera from the plankton, periphyton and benthos of continental waters. Oecologia 19: 75–97.

Hall, D. J., S. T. Threlkeld, C. W. Burns & P. H. Crowley, 1976. The size-efficiency hypothesis and the size structure of zooplankton communities. Annual Review of Ecology and Systematics 7: 177–208.

Hillebrand, H., C. D. Dürselen, D. Kirschtel, U. Pollingher & T. Zohary, 1999. Biovolume calculation for pelagic and benthic microalgae. Journal of Phycology 35: 403–424.

Lawrence, S. G., D. F. Malley, W. J. Findlay, M. A. MacIver & I. L. Delbaere, 1987. Method for estimating dry weight of freshwater planktonic crustaceans from measures of length and shape. Canadian Journal of Fisheries and Aquatic Science 44: 264–274.

McCauley, E., 1984 The estimation of the abundance and biomass of zooplankton in samples. In: Downing, J. A. & F. H. Rigler (Eds) A Manual on Methods for the Assessment of Secondary Productivity in Fresh Waters. Blackwell Scientific Publications, Oxford, pp. 228–265.

McNabb, C. D., 1960. Enumeration of freshwater phytoplankton concentrated on the membrane filter. Limnology and Oceanography 5: 57–61.

terBraak, C. J. F. & P. F. M. Verdonschot. 1995. Canonical correspondence analysis and related multivariate methods in aquatic ecology. Aquatic Sciences 57: 256–288.

Utermöhl, H. 1958. Zur vervollkommnung der quantitativen phytoplankton-methodik: Mit 1 Tabelle und 15 abbildungen im Text und auf 1 Tafel. Internationale Vereinigung für theoretische und angewandte Limnologie: Mitteilungen 9: 1–38.

Wacklin, P., L. Hoffmann & J. Komárek, 2009. Nomenclatural validation of the genetically revised cyanobacterial genus *Dolichospermum* (Ralfs ex Bornet et Flahault) comb. nova. Fottea 9: 59–64.

Womersley, H. B. S. 1984. The marine benthic flora of Southern Australia. Part 1. *University of Adelaide, South Australia*, 329 pp.